

1 **Imaging of porphyrin-specific fluorescence in pathogenic bacteria *in***  
2 ***vitro* using a wearable, hands-free system**

3 Junhong Sun<sup>1,#</sup>, Sangeevan Vellappan<sup>1,2,#</sup>, Johnathan Akdemir<sup>2</sup>, Liviu Steier<sup>3</sup>, Richard E.  
4 Feinbloom<sup>4,5</sup>, Srujana S. Yadavalli<sup>1,2\*</sup>

5 <sup>1</sup>Waksman Institute of Microbiology, Rutgers University, Piscataway, NJ USA

6 <sup>2</sup>Department of Genetics, School of Arts and Sciences, Rutgers University, Piscataway, NJ USA

7 <sup>3</sup>Department of Preventive and Restorative Sciences, Robert Schattner Center, School of  
8 Dental Medicine, University of Pennsylvania, Philadelphia, PA USA

9 <sup>4</sup>Designs for Vision, Inc., Bohemia, NY USA

10

11 #These two authors contributed equally to this work

12

13 \*Corresponding author

14 Waksman Institute of Microbiology

15 Rutgers University

16 190 Frelinghuysen Rd

17 Piscataway NJ 08854

18 Phone: 848-445-0251

19 Email: [sam.yadavalli@rutgers.edu](mailto:sam.yadavalli@rutgers.edu)

20

21 Short title: Porphyrin-specific fluorescence in pathogenic bacteria

22

23 **Keywords:** Bacteria, porphyrins, fluorescence, fluorescence imaging, wearable technology

24

25

## 26 **Highlights**

- 27 • Fluorescence imaging detects porphyrins in bacteria via natural fluorescence.
- 28 • A lightweight, hands-free device enables rapid, non-invasive clinical assessments.
- 29 • The study tested 15 bacterial and 2 fungal strains for porphyrin-based autofluorescence.
- 30 • 14 bacteria fluoresced on Porphyrin Test Agar, 9 on blood agar plates.
- 31 • The REVEAL system aids in diagnosing infections and guiding real-time treatments.

32

## 33 **Abstract**

34 Fluorescence imaging is an effective method for detecting porphyrin production in bacteria,  
35 leveraging the natural fluorescence properties of porphyrins. Here we use a simple, lightweight,  
36 hands-free device for rapid, non-invasive assessments in clinical settings, microbial research,  
37 and diagnostic applications. Specifically in this study, we examined 15 bacterial and 2 fungal  
38 strains commonly associated with skin, oral, and/or multi-site infections at wound sites for their  
39 ability to autofluoresce based on their porphyrin production. We utilized Remel Porphyrin Test  
40 Agar and blood agar plates to monitor red fluorescence over several days of growth under  
41 aerobic or anaerobic conditions using the wearable REVEAL FC imaging system with a 405 nm  
42 violet excitation headlight paired with eyewear carrying 430 nm emission lenses. Fourteen of the  
43 fifteen bacteria produced red fluorescence when grown on Porphyrin Test Agar and nine of the  
44 fifteen bacteria also displayed red fluorescence on blood agar plates, consistent with their ability  
45 to synthesize porphyrins. Taken together, our results elucidate the sensitivity, effectiveness, and  
46 convenience of using wearable technology to detect pathogens that produce porphyrin-specific  
47 fluorescence. Consequently, the REVEAL system has immense potential to help diagnose  
48 wound infections, direct clinical procedures, and guide treatment options in real-time using  
49 fluorescence imaging all while minimizing the risk of contamination.

50

## 51 **1. Introduction**

52 Microbial infections pose significant threats, especially in wound healing (1, 2). If ignored or not  
53 treated promptly, the infection may advance from initial contamination to colonization, local  
54 infection, and even systemic infection, potentially leading to severe conditions like sepsis and  
55 multiple organ dysfunction syndrome (2). In cases such as the infection in diabetic foot ulcers,  
56 timely detection is crucial to prevent potential complications like amputation (3). Similarly,  
57 disregarding the initial stages of dental plaque accumulation in the oral cavity can trigger oral  
58 health complications, such as gingivitis, periodontitis, dental caries, and even tooth loss (4).  
59 Notably, approximately 47.2% of individuals aged 30 years and older are affected by some form  
60 of periodontal disease (4).

61  
62 Considering the rapid spread of infections, when possible, timely detection and effective  
63 management are crucial to prevent infections from progressing to severe stages and reduce the  
64 risk of complications, such as tissue necrosis and the need for amputation (5, 6). Traditional  
65 methods of detecting and confirming bacterial infections, such as culturing and susceptibility  
66 testing, are laborious and time-consuming, taking days to yield results (7). In recent years, there  
67 has been a development of fluorescence-based approaches for real-time visualization of  
68 intrinsic fluorescence from porphyrins produced in bacteria in wound sites and oral plaques,  
69 enabling earlier detection (8–11). Fluorescence-based detection of bacteria relies on the  
70 production of porphyrins, a crucial metabolic intermediate essential for heme biosynthesis and  
71 various biological processes (12). Heme, synthesized by pathogens or obtained from host  
72 sources during infection, plays a pivotal role in energy generation through the electron transport  
73 chain (12). Heme biosynthesis is vital to both aerobic and anaerobic respiration in prokaryotes  
74 (13). In laboratory settings, heme precursors can be provided to microorganisms through  
75 specialized media like porphyrin test agar, or blood agar enriched with 5% sheep's blood cells

76 (14, 15). As pathogens synthesize porphyrins, exposure to violet light (~400-450 nm) leads to  
77 their excitation, emitting light at distinct wavelengths within the red fluorescence at 620-630 nm  
78 (16, 17). Like porphyrin, pyoverdines are siderophores uniquely produced by *Pseudomonas*  
79 *spp.* for iron acquisition, which can be visualized in cyan spectral bands (18). This fluorescence  
80 emission facilitates identifying and visualizing pathogens, thereby enhancing diagnostic  
81 procedures.

82

83 Currently, the real-time fluorescence-guided detection of pathogens uses a handheld device (8).  
84 Serena and colleagues suggest that the use of fluorescence imaging has resulted in changes to  
85 69% of the treatment plans and most importantly, there has been a significant improvement in  
86 patient care in 90% of study wounds (19). This comes as a great benefit to the patient and the  
87 clinician. However, as this technology requires a clinician to use both hands, it hampers the  
88 clinician's ability to provide treatment during real-time fluorescence visualization. The adoption  
89 cost of this technology requires capital expenditure and incurs ongoing operational costs that  
90 limit adoption. Hence, there is a need to develop alternative tools to the existing non-wearable  
91 methods, which can allow for rapid and non-invasive assessment.

92

93 In this study, we report on a new, wearable/ hands-free fluorescence visualization technology  
94 (REVEAL FC wearable imaging system, Design for Vision Inc., Fig 1a) that will enable clinicians  
95 to evaluate the infection at the wound site based on real-time visualization of pathogens and  
96 simultaneously make active treatment decisions. Specifically, we sought to test and characterize  
97 porphyrin detection *via* autofluorescence *in vitro* for some of the common pathogens involved in  
98 skin, oral, and other (respiratory, intestinal, urinary tracts, or blood) infections over a period of  
99 multiple days. We included 15 bacteria and 2 fungi in our analysis. Our results indicate the  
100 ability of REVEAL FC to visualize porphyrin-specific red-orange or pink fluorescence in 14 of the  
101 17 strains tested on porphyrin test agar (Fig 1b). Moreover, we also observed a fluorescence

102 signal for 9 of the 17 strains grown on blood agar plates, suggesting a strong potential for the  
103 detection of microbial infections in wound sites in a clinical setting using the REVEAL FC  
104 wearable technology.

105

## 106 **2. Materials and Methods**

### 107 **2.1. Strains**

108 *E. coli* K-12 MG1655 strain is from the Yadavalli lab collection. The following strains,  
109 *Pseudomonas aeruginosa* PAO1, *Klebsiella pneumoniae* ATCC 13883, *Staphylococcus aureus*  
110 USA300\_LAC, a community-acquired MRSA strain, and *S. Typhimurium* 14028, were gifts from  
111 Drs. Bryce Nickels (Rutgers), Huizhou Fan (Rutgers), Jeffrey Boyd (Rutgers), and Dieter  
112 Schifferli (University of Pennsylvania). All other bacterial and fungal strains used in the study  
113 were purchased from the American Type Culture Collection (ATCC). See Table S1 for additional  
114 details on the bacterial and fungal strains used in this study.

115

### 116 **2.2. Media and growth conditions**

117 For routine growth, bacterial and fungal strains were cultured in liquid or solid agar medium,  
118 either aerobically or anaerobically depending on the organism as specified in Table S1. Agar  
119 plates and culture tubes were then incubated at 37°C with aeration (for aerobic growth) or an  
120 anaerobic growth chamber (for anaerobic growth), depending on a given strain's specific growth  
121 requirement.

122

123 To assess porphyrin production and monitor the associated fluorescence, the strains were  
124 streaked out and grown on Remel Porphyrin Test Agar (PTA, Thermo Fisher Scientific), and/or  
125 blood agar (BA, tryptic soy agar with 5% sheep blood, Thermo Fisher Scientific). Note that both  
126 PTA and BA plates contain heme precursors. For strains grown aerobically, PTA and BA plates

127 were incubated for 5 days at 37°C. Plates were pulled out for imaging daily and returned to  
128 incubation until day 5. For anaerobic strains, PTA and BA plates were incubated for 10 days in  
129 the anaerobic growth chamber, including one plate per strain for each time point (days 2, 4, 7,  
130 and 10) to be pulled out for imaging. At the indicated time points, plates were imaged using the  
131 REVEAL FC technology as described below.

132

### 133 **2.3. Fluorescence imaging**

134 For strains grown aerobically, imaging was performed daily from day 1 to 5. For strains grown in  
135 the anaerobic chamber, one plate corresponding to each strain was removed from the chamber  
136 on days 2, 4, 7, and 10, and imaged. Fluorescence visualization and imaging were performed  
137 using the REVEAL FC, a wearable system equipped with the following: a 405 nm headlight for  
138 excitation, an observational eyewear with an emission filter at 430 nm, a rechargeable power  
139 pack (2 included) with 9 hours of runtime per pack, a smart device attachment for simple and  
140 easy documentation. For this study, a smartphone adapter with a 430 nm emission filter was  
141 attached to an Apple iPhone 12 to capture the images. The images were taken in a dark room.  
142 Images were analyzed and processed using ImageJ (20).

143

## 144 **3. Results**

### 145 **3.1. REVEAL FC imaging system for *in vitro* visualization and imaging of microbial** 146 **fluorescence**

147 Fluorescence visualization requires an excitation source and an emission filter to eliminate the  
148 excitation illumination to maximize the observation of the fluorescent response. The REVEAL  
149 FC developed by Designs for Vision Inc. is a wearable system that is composed of a headlight  
150 that provides excitation and observational eyewear that includes the emission filter (Fig 1). It is  
151 well documented that porphyrins fluoresce when exposed to light in the 400-409nm range (21).

152 Porphyrins are produced as by-products by several microorganisms, including pathogens of  
153 interest. The REVEAL FC headlight utilizes an LED at 405 nm wavelength. Even though the  
154 peak of this LED is at 405nm, well within the excitation range of porphyrins, LEDs are relatively  
155 unfocused. The LED has a wide spectral bandwidth with a transmission range (~380 – 450 nm)  
156 that is too broad for specific excitation of porphyrins (Fig S1) and the spot is too wide to respond  
157 to lensing. The REVEAL FC system uses proprietary and patented technology involving short  
158 wave pass edge filters (shortpass filters) to narrow the spectral bandwidth. Focusing the energy  
159 of the LED to a fixed spot provides uniform illumination within the wavelengths that strongly  
160 excite porphyrins (400 – 425 nm) while eliminating unnecessary wavelengths that could inhibit  
161 the visualization of the fluorescence response. The emission filter is incorporated into a pair of  
162 glasses, which removes all wavelengths less than 430 nm providing a clear image of the field  
163 with no tinting. All the excitation light is removed by the emission filter observational glasses  
164 allowing maximum visualization of the fluorescence response. For documentation, a  
165 smartphone adapter is provided that contains the same emission filter (Fig 1). This is intended  
166 to be attached to any smart device to document and capture the fluorescent images.

167

### 168 **3.2. Porphyrin-specific fluorescence in bacteria and fungi causing skin infection**

169 We explored the fluorescent characteristics of seven prevalent bacterial species and two fungal  
170 species known for causing skin infections or thriving on open skin wounds using the REVEAL  
171 FC system. Among the bacteria tested, three are Gram-positive (*S. aureus*, *C. minutissimum*, *C.*  
172 *acnes*) while the remaining four, *A. hydrophila*, *S. marcescens*, *V. vulnificus* and *P.aeruginosa*  
173 are Gram-negative (Table 1). These bacterial strains were grown aerobically except for *C.*  
174 *acnes*, which is an obligate anaerobe. All of them demonstrate red fluorescence to different  
175 extents as monitored over several days and described below (Table 1, Fig 2).

176

177 In aerobic growth, all bacterial species exhibited fluorescence, while the fungi did not (Table 1,  
178 Fig 2a). *Staphylococcus aureus* displayed intense red fluorescence on porphyrin test agar  
179 (PTA) from day 1, maintaining its intensity through day 5. No fluorescence was observed on  
180 blood agar (BA), whose base is tryptic soy medium (Table S1) that is known to exhibit  
181 background fluorescence that can mask the porphyrin-specific signal (8). Through the Boyd lab  
182 at Rutgers, we had access to *S. aureus hemB* mutant strain, which is deficient in heme  
183 acquisition and porphyrin production (22). Consistently, *S. aureus hemB* mutant showed no  
184 fluorescence throughout the five days, serving as a negative control (8). *Serratia marcescens*  
185 also showed fluorescence on both PTA where the red fluorescence was visible from day 1,  
186 intensifying with each passing day until day 5. On BA, *S. marcescens* seemed to show a faint  
187 pink fluorescence on day 1, though there was no signal on days 2 and 5. *Corynebacterium*  
188 *minutissimum* exhibited red fluorescence on PTA starting from day 1, with increased intensity on  
189 days 2 and 3, persisting at least until day 5 when all colonies exhibited red fluorescence.  
190 Interestingly, we detected red fluorescence for *C. minutissimum* on BA from day 1, reaching  
191 maximum intensity by days 2-3, which indicates a signal higher than the background for BA and  
192 the fluorescence diminished by day 5. Similarly, for *Vibrio vulnificus*, bright red fluorescence was  
193 visible on days 1 and 2, gradually diminishing by days 3 and 5. On BA, *V. vulnificus* showed red  
194 fluorescence as observed on days 1 and 2, with the intensity decreasing and nearly  
195 disappearing by day 5. *Aeromonas hydrophila* displayed red fluorescence on PTA from day 1,  
196 intensifying remarkably by day 2 and the bright red signal stayed steady until day 5. Similar to  
197 *C. minutissimum* and *V. vulnificus*, we observed red fluorescence for *A. hydrophila* on BA but  
198 with a delayed appearance on day 2, progressively intensifying by day 5. *Pseudomonas*  
199 *aeruginosa* exhibited red fluorescence on PTA, with a weak signal on day 1, transitioning to a  
200 brighter red signal by day 2 and continuing into day 5 (Fig 2a). On BA, *P. aeruginosa* exhibited  
201 cyan fluorescence on day 1, persisting until day 5. *Pseudomonas spp.* are known to synthesize



202 a variety of phenazine pigments including pyoverdines (23), which contribute to the observed  
203 cyan fluorescence in our *P. aeruginosa* PAO1 strain.

204

205 The fluorescence changes in anaerobes were observed over a longer period, extending up to  
206 10 days, due to their slower growth rate. *Cutibacterium acnes*, an aerotolerant anaerobe (24),  
207 exhibited fluorescence on both PTA and BA (Fig 2b). It displayed red fluorescence from day 2,  
208 intensifying by day 4 and reaching peak intensity around day 7, but the fluorescence intensity  
209 reduced on day 10. On BA, very faint red fluorescence was observed on day 2, which is more  
210 evident on day 4, intensifying by day 7, and diminished by day 10. Fungal strains *Candida*  
211 *albicans* and *Malassezia furfur* did not show red fluorescence, which is consistent with previous  
212 studies (8) (Fig 2c).

213

### 214 **3.3. Porphyrin-specific fluorescence in bacteria causing oral infection**

215 We examined two bacterial pathogens known for causing oral infections: *Streptococcus mutans*,  
216 a Gram-positive bacterium typically inhabiting dental plaque (25), and *Porphyromonas*  
217 *gingivalis*, a Gram-negative obligate anaerobe associated with pulpal infections, oral abscesses,  
218 and periodontitis (26). *S. mutans* showed no fluorescence under aerobic growth but appeared to  
219 show a faint orange signal under anaerobic conditions (Table 1, Fig 3). The second oral  
220 pathogen, *P. gingivalis* formed red colonies on PTA, beginning as early as day 2 and 4, but  
221 diminishing by day 7 and becoming less visible by day 10 (Fig 3b). On BA, it exhibited no  
222 fluorescence on day 2 but developed red fluorescence by day 4. By day 7 on BA, there is a  
223 reduction in the red fluorescence and *P. gingivalis* starts to show black pigmentation, which is  
224 more prominent by day 10 (Fig 3b). The black-pigmented colonies on blood agar are associated  
225 with the accumulation of heme complexes as noted previously (27).

226

### 227 **3.4. Porphyrin-specific fluorescence in bacteria causing multi-site/other infections**

228 In this section, we tested six bacterial strains that exhibit a diverse range of pathogenic  
229 behaviors across distinct anatomical sites and not being exclusively confined to cutaneous or  
230 oral infection (Table 1). Two of the six bacterial strains are Gram-positive, while the remaining  
231 four are Gram-negative. Five of these species (*Listeria monocytogenes*, *Escherichia coli*,  
232 *Klebsiella pneumoniae*, *Salmonella typhimurium*, and *Proteus mirabilis*) demonstrate  
233 fluorescence under aerobic conditions, whereas one (*Streptococcus pyogenes*) exhibits  
234 fluorescence exclusively under anaerobic conditions (Fig 4).

235  
236 Under aerobic growth conditions, *S. pyogenes*, a facultative anaerobe (28), did not exhibit any  
237 fluorescence on PTA (Fig 4a). However, when *S. pyogenes* was grown under anaerobic growth  
238 conditions, red fluorescence was readily visible from day 2 and persisted through days 4, 7, and  
239 10 on both PTA and BA (Fig 4b). *L. monocytogenes* exhibited fluorescence on PTA from day 1,  
240 intensifying by day 2 with a slight reduction in intensity by day 5 (Fig 4a). Three strains, *E. coli*,  
241 *K. pneumoniae*, and *S. typhimurium* displayed red fluorescence from day 1 with an increased  
242 intensity on day 2, which remained strong and stable through day 5. Intriguingly, *P. mirabilis*  
243 exhibited bright pink fluorescence on PTA on day 1, intensifying on days 2 and 3, but reducing  
244 in intensity by day 5. On BA, *P. mirabilis* showed cyan fluorescence, which was visible on day 1,  
245 gradually intensifying by day 3 and remaining consistent thereafter. Secondary metabolites such  
246 as phenazines are thought to be produced by a variety of bacteria (29) and the cyan  
247 fluorescence observed here for *P. mirabilis* grown on BA may be due to the accumulation of a  
248 pyoverdine-like pigment.

249

#### 250 **4. Discussion and conclusions**

251 Wearable technology in clinical practice and diagnostics encompasses devices such as  
252 smartwatches, fitness trackers, smart clothing, and implantable sensors, which collect data on

253 various physiological parameters such as heart rate, activity levels, sleep patterns, blood  
254 glucose levels, and more (30, 31). These devices have a broad scope of applications in  
255 monitoring chronic conditions, fitness, wellness, rehabilitation, clinical trials, and mental health  
256 as well as early diagnosis and prevention. Additionally, there has been progress in developing  
257 wearable devices for clinicians and healthcare professionals ranging from smartwatches and  
258 augmented reality glasses to biometric sensors to enhance diagnosis, surgical planning,  
259 precision, and hands-free communication (32, 33).

260

261 In this study, we use the REVEAL FC imaging system developed by Designs for Vision Inc., a  
262 lightweight and comfortable hands-free device that can be customized to the operator's ocular  
263 specifications (Fig 1, S1). It minimizes cross-contamination risks and enhances objective  
264 assessment capabilities, overcoming limitations posed by bulky and tedious traditional tools.  
265 Here we systematically analyzed 15 bacterial and 2 fungal pathogens (Table 1, S1) for red  
266 fluorescence associated with porphyrin production *in vitro* under aerobic (days 1 through 5) or  
267 anaerobic (days 2 through 10) growth conditions. By plating strains on porphyrin test agar  
268 (PTA), we detected a strong red fluorescent signal in all but one (*S. mutans*) of the bacterial  
269 strains tested. *S. pyogenes* displayed red fluorescence but only under anaerobic growth  
270 conditions. Two other *Streptococcus* strains do not display red fluorescence as documented  
271 previously (8), and some bacteria from this genus are known to be deficient in heme  
272 biosynthesis (12, 34). Remarkably, red fluorescence has been reported for *S. mutans* in a  
273 dentin caries model pointing to a potential media- and context-dependent mechanism for  
274 porphyrin production in this bacterium (35).

275

276 For a majority of the bacterial strains, the signal was evident by day 1 and in a few cases,  
277 depending on the individual bacterial strain, there was a delayed onset of fluorescence. We also  
278 plated the strains on blood agar and found that 9 of the 15 bacteria displayed red fluorescence.

279 It is worth noting that the tryptic soy blood agar medium has background fluorescence that  
280 typically masks any signal from the bacteria, however, REVEAL was able to detect the red  
281 signal above the threshold of the background, suggesting that this system is highly sensitive.  
282 Unsurprisingly, the two fungal strains included in this study, *C. albicans* and *M. furfur* did not  
283 show porphyrin-dependent red fluorescence, suggesting that they may not produce heme and  
284 instead acquire heme from their environments (36).

285  
286 This method, like other porphyrin-based approaches, is limited by the fact that not all bacteria  
287 produce porphyrins. Internal and external factors can also impact porphyrin production, affecting  
288 detection. While the in vitro agar plate model may not fully replicate real-world infection  
289 conditions, it provides a foundational step to guide clinicians.

290  
291 Overall, wearable technology for healthcare professionals enhances medical practice by  
292 enabling faster detection and intervention, improving patient care, increasing efficiency, and  
293 supporting more informed clinical decision-making. The use of wearable technology is directly  
294 linked to improved patient outcomes in clinical settings (37). For instance, the detection of  
295 bacteria in the oral cavity plays a crucial role in diagnosing and treating infections, as they serve  
296 as indicators for infected tissue and dental plaque (15). Previous work has shown that  
297 fluorescence imaging using the REVEAL system can help with diagnosis and treatment  
298 guidance in cariology, oral hygiene, and peri-implantitis (35, 38–40).

299  
300 More broadly, the smart wearable fluorescence imaging system described here has immense  
301 potential for diagnosis, treatment, and many other applications across pharmaceutical,  
302 healthcare, food, and agricultural industries.

303

## 304 **Acknowledgement**

305 We thank Drs. Meliza Talaue, Xuesong Zhang, and Dr. Martin Blaser's laboratory at the Center  
306 for Advanced Biotechnology and Medicine at Rutgers University for the access and use of an  
307 anaerobic chamber.

308

## 309 **Funding**

310 This work was supported by funding from different sources - the National Institutes of Health -  
311 National Institute of General Medical Sciences (NIH-NIGMS) ESI-MIRA R35 GM147566 and  
312 institutional start-up funds from Rutgers (to S.S.Y.) and financial support from Designs for  
313 Vision, Inc. The funders did not play a role in the study design, data collection and analysis,  
314 decision to publish, or preparation of the manuscript.

315

## 316 **Ethics statement**

317 This study did not include human samples. The use of human pathogens in the licensed BSL-2  
318 laboratory was approved by the institutional biosafety committee. All biosafety regulations were  
319 followed during the conduct of this study.

320

## 321 **Declaration of generative AI in scientific writing**

322 The current version of ChatGPT (GPT-4o) was used to improve the readability and clarity in the  
323 abstract and introductory sections of this paper. The authors declare that generative AI was not  
324 used for scientific writing or in creating figures or images included in the manuscript.

325

## 326 **CRedit authorship contribution statement**

327 Junhong Sun: Data curation, Investigation, Validation. Sangeevan Vellappan: Data curation,  
328 Visualization, Writing- Original draft preparation. Johnathan Akdemir: Data curation,  
329 Visualization. Liviu Steier: Methodology, Resources. Richard E. Feinbloom: Methodology,  
330 Resources. Srujana S. Yadavalli: Conceptualization, Funding acquisition, Supervision, Writing-  
331 Original draft preparation, Writing- Reviewing and Editing.

332

### 333 **Declaration of competing interest**

334 The authors J.S., S.V., J. A., declare no competing interests. S.S.Y. collaborates with Designs  
335 for Vision, Inc. R.E.F. is the President Designs for Vision, Inc., and L.S. holds IP rights and  
336 receives royalties on Reveal.

337

### 338 **Data Availability Statement**

339 The authors declare that all data supporting the findings of this study are available within the  
340 main article and its supplementary information files.

341

### 342 **References**

- 343 1. Monika P, Chandrababha MN, Rangarajan A, Waiker PV, Chidambara Murthy KN. 2021.  
344 Challenges in Healing Wound: Role of Complementary and Alternative Medicine. *Front Nutr*  
345 8:791899.
- 346 2. Leaper D, Assadian O, Edmiston CE. 2015. Approach to chronic wound infections. *Br J*  
347 *Dermatol* 173:351–358.
- 348 3. Gardner SE, Hillis SL, Frantz RA. 2009. Clinical signs of infection in diabetic foot ulcers with  
349 high microbial load. *Biol Res Nurs* 11:119–128.

- 350 4. Eke PI, Dye BA, Wei L, Thornton-Evans GO, Genco RJ, CDC Periodontal Disease  
351 Surveillance workgroup: James Beck (University of North Carolina, Chapel Hill, USA),  
352 Gordon Douglass (Past President, American Academy of Periodontology), Roy Page  
353 (University of Washin. 2012. Prevalence of periodontitis in adults in the United States: 2009  
354 and 2010. *J Dent Res* 91:914–920.
- 355 5. Aydin SY, Ercan A, Ercan D. 2023. Investigation of the effects of clinical parameters on  
356 mortality in patients with necrotizing fasciitis. *Ulus Travma Acil Cerrahi Derg* 29:1150–1157.
- 357 6. Ahluwalia RS, Reichert ILH. 2021. Surgical management of the acute severely infected  
358 diabetic foot - The “infected diabetic foot attack”. An instructional review. *J Clin Orthop*  
359 *Trauma* 18:114–120.
- 360 7. Avershina E, Khezri A, Ahmad R. 2023. Clinical Diagnostics of Bacterial Infections and  
361 Their Resistance to Antibiotics-Current State and Whole Genome Sequencing  
362 Implementation Perspectives. *Antibiotics (Basel)* 12.
- 363 8. Jones LM, Dunham D, Rennie MY, Kirman J, Lopez AJ, Keim KC, Little W, Gomez A,  
364 Bourke J, Ng H, DaCosta RS, Smith AC. 2020. In vitro detection of porphyrin-producing  
365 wound bacteria with real-time fluorescence imaging. *Future Microbiol* 15:319–332.
- 366 9. Lopez AJ, Jones LM, Reynolds L, Diaz RC, George IK, Little W, Fleming D, D’souza A,  
367 Rennie MY, Rumbaugh KP, Smith AC. 2021. Detection of bacterial fluorescence from in  
368 vivo wound biofilms using a point-of-care fluorescence imaging device. *Int Wound J*  
369 18:626–638.
- 370 10. Shakibaie F, Lamard L. 2018. Application of fluorescence spectroscopy for microbial  
371 detection to enhance clinical investigations. *Photon Counting*.

- 372 11. Koenig K, Schneckenburger H, Hemmer J, Tromberg BJ, Steiner RW. 1994. In-vivo  
373 fluorescence detection and imaging of porphyrin-producing bacteria in the human skin and  
374 in the oral cavity for diagnosis of acne vulgaris, caries, and squamous cell carcinoma, p.  
375 129–138. *In Advances in Laser and Light Spectroscopy to Diagnose Cancer and Other*  
376 *Diseases*. SPIE.
- 377 12. Choby JE, Skaar EP. 2016. Heme Synthesis and Acquisition in Bacterial Pathogens. *J Mol*  
378 *Biol* 428:3408–3428.
- 379 13. Layer G. 2021. Heme biosynthesis in prokaryotes. *Biochim Biophys Acta Mol Cell Res*  
380 1868:118861.
- 381 14. Gadberry JL, Amos MA. 1986. Comparison of a new commercially prepared porphyrin test  
382 and the conventional satellite test for the identification of *Haemophilus* species that require  
383 the X factor. *J Clin Microbiol* 23:637–639.
- 384 15. Lennon ÁM, Brune L, Techert S, Buchalla W. 2023. Fluorescence Spectroscopy Shows  
385 Porphyrins Produced by Cultured Oral Bacteria Differ Depending on Composition of Growth  
386 Media. *Caries Res* 57:74–86.
- 387 16. Gouterman M. 1961. Spectra of porphyrins. *J Mol Spectrosc* 6:138–163.
- 388 17. Case N, Johnston N, Nadeau J. 2024. Fluorescence microscopy with deep UV, near UV,  
389 and visible excitation for in situ detection of microorganisms. *Astrobiology* 24:300–317.
- 390 18. Schalk IJ, Guillon L. 2013. Pyoverdine biosynthesis and secretion in *Pseudomonas*  
391 *aeruginosa*: implications for metal homeostasis. *Environ Microbiol* 15:1661–1673.
- 392 19. Le L, Baer M, Briggs P, Bullock N, Cole W, DiMarco D, Hamil R, Harrell K, Kasper M, Li W,  
393 Patel K, Sabo M, Thibodeaux K, Serena TE. 2021. Diagnostic Accuracy of Point-of-Care



- 394 Fluorescence Imaging for the Detection of Bacterial Burden in Wounds: Results from the  
395 350-Patient Fluorescence Imaging Assessment and Guidance Trial. *Adv Wound Care*  
396 10:123–136.
- 397 20. Schneider CA, Rasband WS, Eliceiri KW. 2012. NIH Image to ImageJ: 25 years of image  
398 analysis. *Nat Methods* 9:671–675.
- 399 21. Teixeira R, Serra VV, Botequim D, Paulo PMR, Andrade SM, Costa SMB. 2021.  
400 Fluorescence Spectroscopy of Porphyrins and Phthalocyanines: Some Insights into  
401 Supramolecular Self-Assembly, Microencapsulation, and Imaging Microscopy. *Molecules*  
402 26.
- 403 22. Granick S, Beale SI. 1978. Hemes, chlorophylls, and related compounds: biosynthesis and  
404 metabolic regulation. *Adv Enzymol Relat Areas Mol Biol* 46:33–203.
- 405 23. Orlandi VT, Martegani E, Bolognese F, Trivellin N, Garzotto F, Caruso E. 2021.  
406 Photoinactivation of *Pseudomonas aeruginosa* Biofilm by Dicationic Diaryl-Porphyrin. *Int J*  
407 *Mol Sci* 22.
- 408 24. Ahle CM, Feidenhansl C, Brüggemann H. 2023. *Cutibacterium acnes*. *Trends Microbiol*  
409 31:419–420.
- 410 25. Lemos JA, Palmer SR, Zeng L, Wen ZT, Kajfasz JK, Freires IA, Abranches J, Brady LJ.  
411 2019. The Biology of *Streptococcus mutans*. *Microbiol Spectr* 7.
- 412 26. Condorelli F, Scalia G, Calì G, Rossetti B, Nicoletti G, Lo Bue AM. 1998. Isolation of  
413 *Porphyromonas gingivalis* and detection of immunoglobulin A specific to fimbrial antigen in  
414 gingival crevicular fluid. *J Clin Microbiol* 36:2322–2325.

- 415 27. Nakayama K. 2015. Porphyromonas gingivalis and related bacteria: from colonial  
416 pigmentation to the type IX secretion system and gliding motility. *J Periodontal Res* 50:1–8.
- 417 28. Gera K, Mclver KS. 2013. Laboratory growth and maintenance of Streptococcus pyogenes  
418 (the Group A Streptococcus, GAS). *Curr Protoc Microbiol* 30:9D.2.1-9D.2.13.
- 419 29. Pierson LS 3rd, Pierson EA. 2010. Metabolism and function of phenazines in bacteria:  
420 impacts on the behavior of bacteria in the environment and biotechnological processes.  
421 *Appl Microbiol Biotechnol* 86:1659–1670.
- 422 30. Williams GJ, Al-Baraikhan A, Rademakers FE, Ciravegna F, van de Vosse FN, Lawrie A,  
423 Rothman A, Ashley EA, Wilkins MR, Lawford PV, Omholt SW, Wisløff U, Hose DR, Chico  
424 TJA, Gunn JP, Morris PD. 2023. Wearable technology and the cardiovascular system: the  
425 future of patient assessment. *Lancet Digit Health* 5:e467–e476.
- 426 31. Mondal S, Zehra N, Choudhury A, Iyer PK. 2021. Wearable Sensing Devices for Point of  
427 Care Diagnostics. *ACS Appl Bio Mater* 4:47–70.
- 428 32. McKnight RR, Pean CA, Buck JS, Hwang JS, Hsu JR, Pierrie SN. 2020. Virtual Reality and  
429 Augmented Reality-Translating Surgical Training into Surgical Technique. *Curr Rev*  
430 *Musculoskelet Med* 13:663–674.
- 431 33. Barteit S, Lanfermann L, Bärnighausen T, Neuhann F, Beiersmann C. 2021. Augmented,  
432 Mixed, and Virtual Reality-Based Head-Mounted Devices for Medical Education:  
433 Systematic Review. *JMIR Serious Games* 9:e29080.
- 434 34. Cavallaro G, Decaria L, Rosato A. 2008. Genome-based analysis of heme biosynthesis and  
435 uptake in prokaryotic systems. *J Proteome Res* 7:4946–4954.

- 436 35. Steier L, Sidhu P, Qasim SS, Mahdi SS, Daood U. 2022. Visualization of initial bacterial  
437 colonization on dentin using fluorescence activating headlight for fluorescence enhanced  
438 theragnosis. *Photodiagnosis Photodyn Ther* 38:102732.
- 439 36. Kornitzer D, Roy U. 2020. Pathways of heme utilization in fungi. *Biochim Biophys Acta Mol*  
440 *Cell Res* 1867:118817.
- 441 37. Slimani A, Terrer E, Manton DJ, Tassery H. 2020. Carious lesion detection technologies:  
442 factual clinical approaches. *Br Dent J* 229:432–442.
- 443 38. Steier L. 2020. Reveal: Fluorescence Enhanced Theragnosis by Designs for Vision. *Eur J*  
444 *Dent* 14:186–188.
- 445 39. Steier L, Figueiredo JAP de, Blatz MB. 2021. Fluorescence-enhanced theragnosis: A novel  
446 approach to visualize, detect, and remove caries. *Compend Contin Educ Dent* 42:460–465.
- 447 40. Hiltch G, Steier L, de Figueiredo JAP. 2023. Enhanced clinical decision-making and  
448 delivery of minimally invasive care using the ICCMS4D integrated with hands-free  
449 fluorescence-based loupes and a chemomechanical caries removal agent. *Eur J Dent*  
450 17:1356–1362.

451

452

453

454

455

456

457

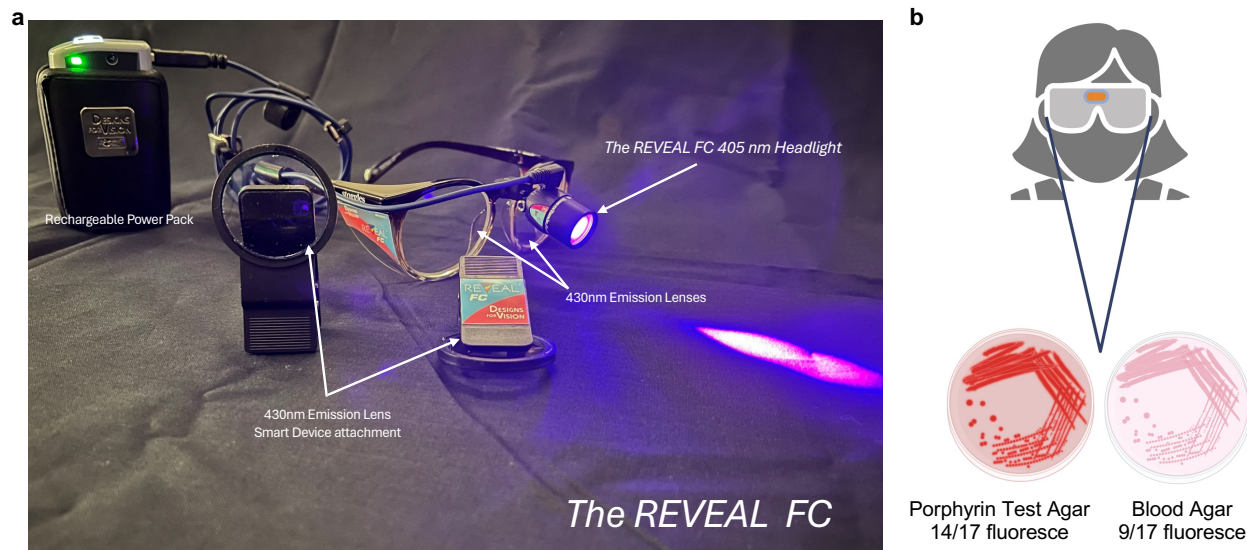
458

459 **Tables, figures, and legends**

460 **Table 1. List of bacterial and fungal strains plated on Porphyrin Test Agar (PTA) or blood**  
 461 **agar (BA) and tested for fluorescence production.**

Strain	Category	Growth	Incubation time in days	Fluorescence	
				PTA	BA
<b>Gram-positive bacteria</b>					
<i>Corynebacterium minutissimum</i>	skin	aerobic	5	Red/orange	Pink
<i>Cutibacterium acnes</i> (previously <i>Propionibacterium acnes</i> )	skin	anaerobic	10	Red	Red
<i>Staphylococcus aureus</i>	skin	aerobic	5	Red	–
<i>Staphylococcus aureus</i> ( $\Delta$ hemB)		aerobic	5	–	–
<i>Streptococcus mutans</i>	oral	aerobic	5	–	–
		anaerobic	10	–	–
<i>Listeria monocytogenes</i>	other (blood)	aerobic	5	Red	–
<i>Streptococcus pyogenes</i>	other (respiratory tract)	anaerobic	10	Red	Red
		aerobic	5	–	–
<b>Gram-negative bacteria</b>					

<i>Aeromonas hydrophila</i>	skin	aerobic	5	Red	Pink
<i>Pseudomonas aeruginosa</i>	skin, multi-site	aerobic	5	Red	Cyan
<i>Serratia marcescens</i>	skin, urinary tract	aerobic	5	Red	Pink
<i>Vibrio vulnificus</i>	skin	aerobic	5	Red	Pink
<i>Porphyromonas gingivalis</i>	oral	anaerobic	10	Red	Red/black
<i>Escherichia coli</i>	other (intestinal, urinary tract)	aerobic	5	Red	-
<i>Klebsiella pneumoniae</i>	other (multi-site)	aerobic	5	Red	-
<i>Proteus mirabilis</i>	other (urinary tract)	aerobic	5	Pink	Cyan
<i>Salmonella typhimurium</i>	other (intestinal tract)	aerobic	5	Red	-
<b>Fungi</b>					
<i>Candida albicans</i>	skin	aerobic	10	-	-
<i>Malassezia furfur</i>	skin	aerobic	10	-	-



463

464

465 **Figure 1. Overview of porphyrin-specific fluorescence detection in pathogenic microbes**

466 **using the REVEAL FC imaging system.** a) The REVEAL FC is a wearable imaging system

467 composed of a headlight that provides excitation at 405 nm and observational eyewear, which

468 includes the emission filter at 430 nm. This system includes a rechargeable power pack and

469 smart device attachment for simple and effective visualization and imaging of microbial

470 samples. b) 17 microbial species (15 bacteria and 2 fungi) commonly associated with skin, oral,

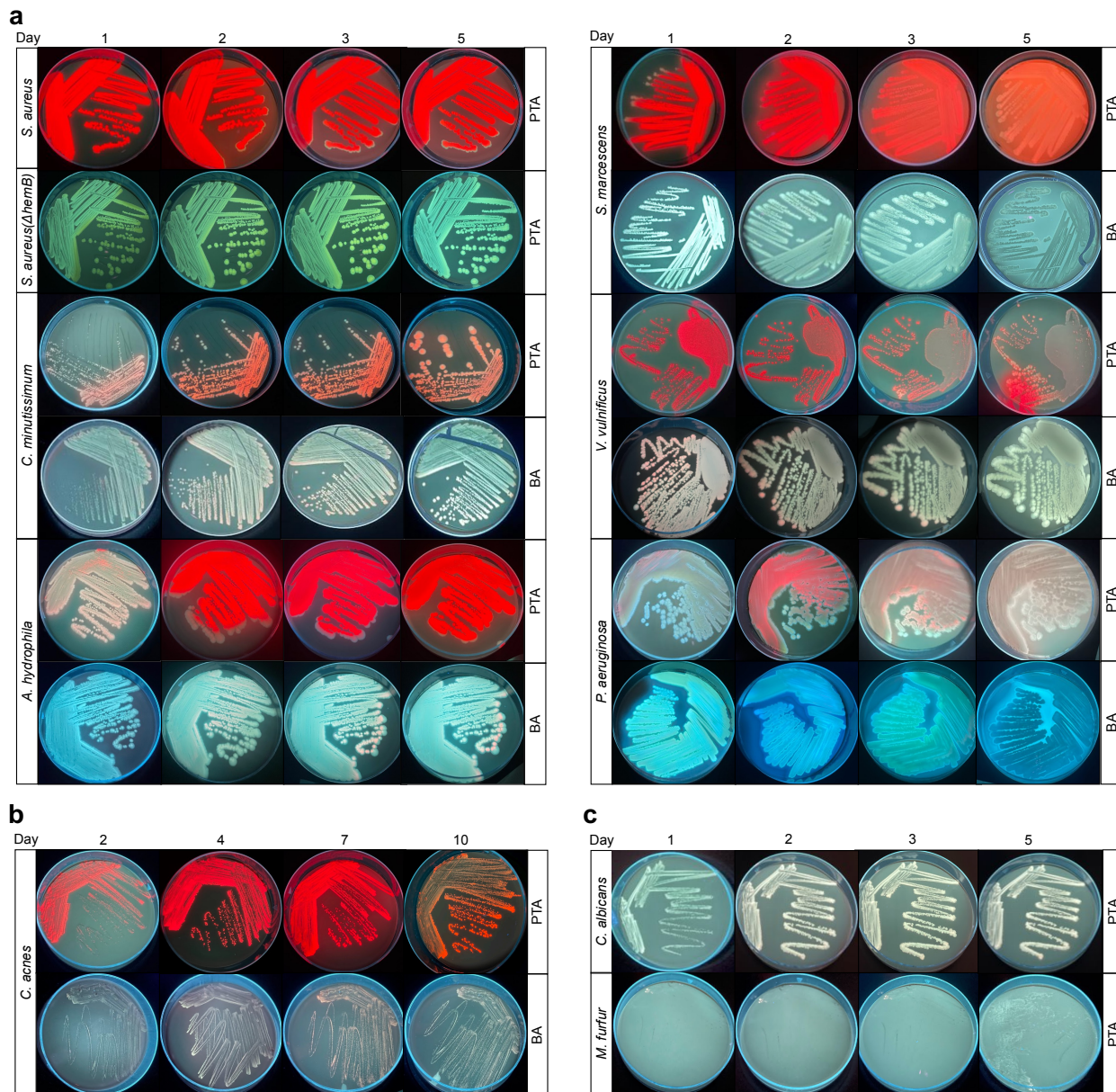
471 and other infections were tested for autofluorescence of porphyrins. 14 of them exhibited

472 fluorescence in shades ranging from red/orange to pink on porphyrin test agar, while 9 of them

473 displayed fluorescence on blood agar.

474

475



476

477

478 **Figure 2. Porphyrin-specific fluorescence detection in microbes associated with skin**

479 **infection.** a) Fluorescence-based imaging of bacteria on porphyrin test agar (PTA) and/or blood

480 agar under aerobic conditions after 1, 2, 3, and 5 days of growth. Bacterial strains

481 *Staphylococcus aureus* and its mutant  $\Delta$ hemB, *Corynebacterium minutissimum*, *Aeromonas*

482 *hydrophila*, *Serratia marcescens*, *Vibrio vulnificus*, and *Pseudomonas aeruginosa* are labeled as

483 *S. aureus*, *S. aureus*  $\Delta$ hemB, *C. minutissimum*, *A. hydrophila*, *S. marcescens*, *V. vulnificus*, and

484 *P. aeruginosa*, respectively. b) Fluorescence-based imaging of bacteria grown on porphyrin test  
485 agar (PTA) and/or blood agar under anaerobic conditions after 2, 4, 7, and 10 days of growth.  
486 The bacterial strain *Cutibacterium acnes* is labeled as *C. acnes*. c) Fluorescence-based imaging  
487 of fungi on porphyrin test agar (PTA) and/or blood agar under aerobic conditions after 1, 2, 3,  
488 and 5 days of growth. Fungal strains *Candida albicans* and *Malassezia furfur* are labeled as *C.*  
489 *albicans* and *M. furfur*, respectively. Images are representative of four biological replicates.

490

491

492

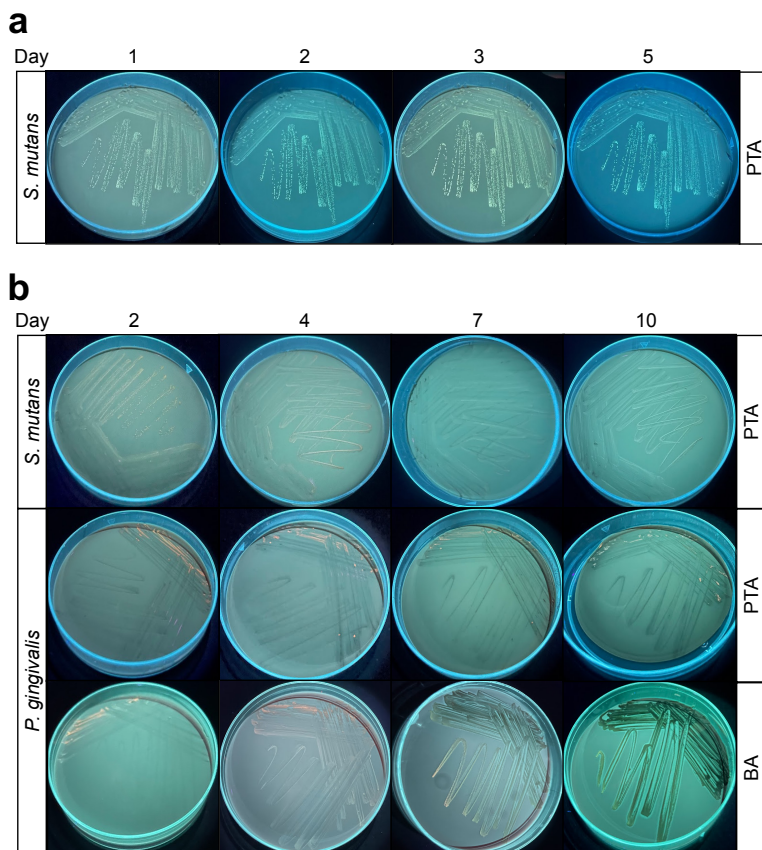
493

494

495

496





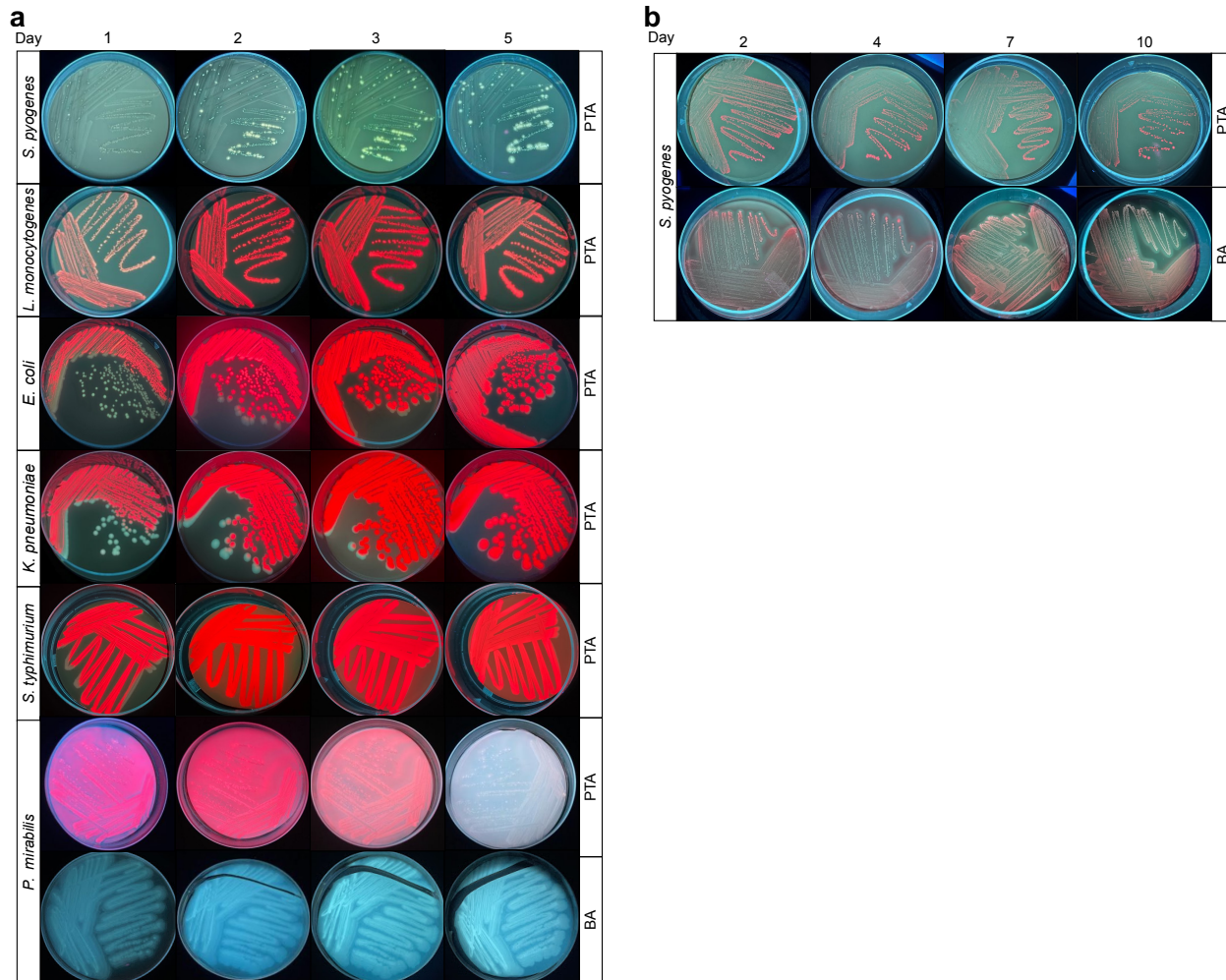
497

498

499 **Figure 3. Porphyrin-specific fluorescence detection in bacteria associated with oral**  
500 **infection.** a) Fluorescence-based imaging of bacteria on porphyrin test agar (PTA) and/or blood  
501 agar under aerobic conditions after 1, 2, 3, and 5 days of growth. The bacterial strain  
502 *Streptococcus mutans* is labeled as *S. mutans*. b) Fluorescence-based imaging of bacteria  
503 grown on porphyrin test agar (PTA) and/or blood agar under aerobic conditions after 2, 4, 7, and  
504 10 days of growth. Bacterial strains *Streptococcus mutans* and *Porphyromonas gingivalis* are  
505 labeled as *S. mutans* and *P. gingivalis*, respectively. Images are representative of four biological  
506 replicates.

507

508



509

510

511 **Figure 4. Porphyrin-specific fluorescence detection in bacteria associated with other**  
512 **infections.** a) Fluorescence-based imaging of bacteria on porphyrin test agar (PTA) and/or  
513 blood agar under aerobic conditions after 1, 2, 3, and 5 days of growth. Bacterial strains  
514 *Streptococcus pyogenes*, *Listeria monocytogenes*, *Escherichia coli*, *Klebsiella pneumoniae*,  
515 *Salmonella typhimurium*, and *Proteus mirabilis* are labeled as *S. pyogenes*, *L. monocytogenes*,  
516 *E. coli*, *K. pneumoniae*, *S. typhimurium*, and *P. mirabilis*, respectively. b) Fluorescence-based  
517 imaging of bacteria grown on porphyrin test agar (PTA) and/or blood agar under aerobic  
518 conditions after 2, 4, 7, and 10 days of growth. The bacterial strain *Streptococcus pyogenes* is  
519 labeled as *S. pyogenes*. Images are representative of four biological replicates.

520 **Supporting Information**

521 **Table S1. List of strains, growth conditions, and liquid culture media used in the study.**

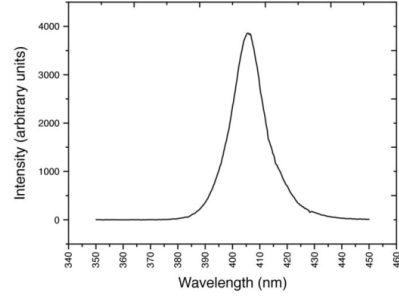
522

Strain	Growth condition and media	Source
<b>Bacteria</b>		
<i>Aeromonas hydrophila</i>	aerobic, 37°C, Tryptic Soy Broth (Avantor)	ATCC 35654
<i>Corynebacterium minutissimum</i>	aerobic, 37°C, Brain Heart Infusion (BD)	ATCC 23348
<i>Cutibacterium acnes</i> (previously <i>Propionibacterium acnes</i> )	anaerobic, 37°C, Tryptic Soy Broth (Avantor)	ATCC 6919
<i>Escherichia coli</i> MG1655	aerobic, 37°C, LB Miller (IBI Scientific)	Yadavalli lab
<i>Klebsiella pneumoniae</i> 13883	aerobic, 37°C, LB Miller (IBI Scientific)	Fan lab
<i>Listeria monocytogenes</i>	aerobic, 37°C, Brain Heart Infusion (BD)	ATCC 19115
<i>Porphyromonas gingivalis</i>	anaerobic, 37°C, Tryptic Soy Broth (Avantor), supplemented with Vitamin K and hemin (BD)	ATCC 33277
<i>Proteus mirabilis</i>	aerobic, 37°C, LB Miller (IBI Scientific)	ATCC 25933
<i>Pseudomonas aeruginosa</i> PAO1	aerobic, 37°C, LB Miller (IBI Scientific)	Nickels lab
<i>Salmonella typhimurium</i> 14028	aerobic, 37°C, LB Miller (IBI Scientific)	Schifferli lab
<i>Serratia marcescens</i>	aerobic, 37°C, LB Miller (IBI Scientific)	ATCC 13880

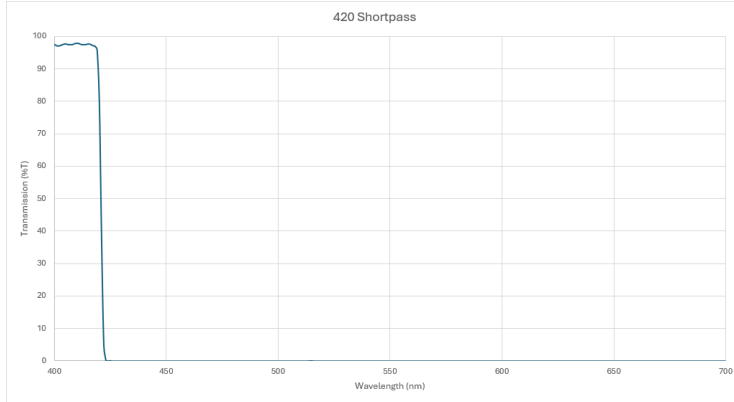
<i>Staphylococcus aureus</i> USA300_LAC (community acquired MRSA strain)	aerobic, 37°C, LB Miller (IBI Scientific)	Boyd lab
<i>Staphylococcus aureus</i> ( $\Delta$ hemB)	aerobic, 37°C, LB Miller (IBI Scientific)	Boyd lab
<i>Streptococcus mutans</i>	aerobic, 37°C, Brain Heart Infusion (BD)	ATCC 35668
	anaerobic, 37°C, Brain Heart Infusion (BD)	
<i>Streptococcus pyogenes</i>	aerobic, 37°C, Brain Heart Infusion (BD)	ATCC 19615
	anaerobic, 37°C, Brain Heart Infusion (BD)	
<i>Vibrio vulnificus</i>	aerobic, 37°C, LB Miller (IBI Scientific)	ATCC 27562
<b>Fungi</b>		
<i>Candida albicans</i>	aerobic, 37°C, Yeast Peptone Dextrose Broth (BD)	ATCC 18804
<i>Malassezia furfur</i>	aerobic, 37°C, Brain Heart Infusion (BD) supplemented with Ox bile (Hardy Diagnostic)	ATCC 14521

523

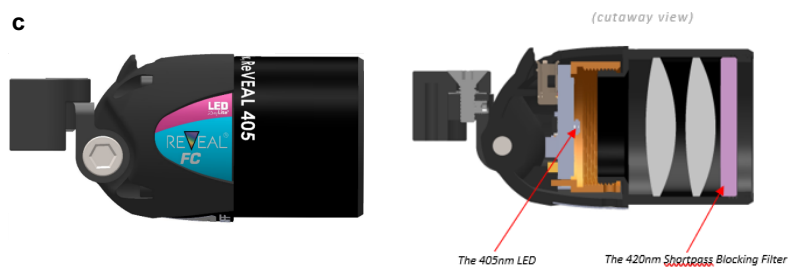
**a** Transmission curve of a 405 nm LED



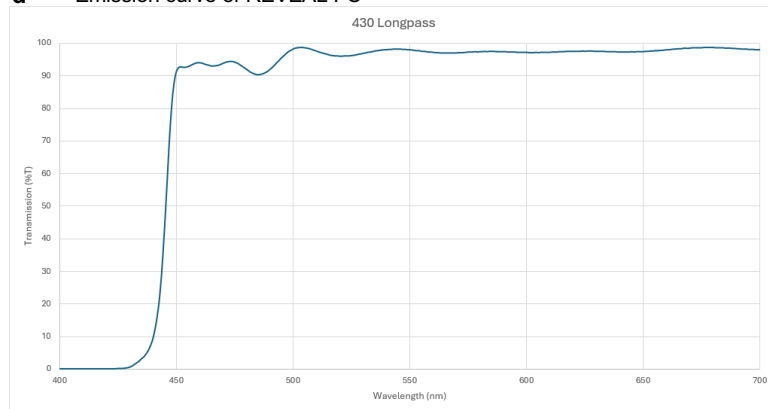
**b** Transmission curve of REVEAL FC



**c**



**d** Emission curve of REVEAL FC



524

525

526 **Figure S1. Fluorescence emission spectra for the 405 nm LED.** a) Representative  
527 transmission curve of a typical 405 nm LED showing light transmission across a range of  
528 wavelengths (380 – 450 nm). b) Transmission curve of REVEAL FC using a 420 nm shortpass  
529 filter focusing fluorescence excitation at 400 – 425 nm. c) Diagram of the REVEAL FC lens with  
530 a cross-sectional depiction of the 405 nm LED and the 420 nm shortpass cut-off filter. d)  
531 Emission curve of REVEAL FC lens showing emission at wavelengths  $\geq 430$  nm.